Available online at www.sciencedirect.com
ScienceDirect
Journal of Sound and Vibration 311 (2008) 1457–1464
JOURNAL OF SOUND AND VIBRATION
www.elsevier.com/locate/jsvi

Short Communication

Critical analysis of analogous mechanical models used to describe hydraulic engine mounts

Jun Hwa Lee, Rajendra Singh*

Acoustics and Dynamics Laboratory, Department of Mechanical Engineering, The Ohio State University, Columbus, OH 43210, USA

Received 4 May 2007; received in revised form 1 October 2007; accepted 12 October 2007
Available online 19 November 2007

Abstract

Passive hydraulic engine mounts differ from mechanical isolators in several ways. Complex poles and zeros suggest that the hydraulic mount has at least one mass (inertia) element even at low frequencies. This would suggest thus that the constraint forces at its input and output ends are not identical; but they are indeed, like any conventional spring. Accordingly, analogous mechanical models of hydraulic mounts, consisting of spring, dashpot and mass elements, could lead to incorrect results in the context of system analysis. Examples clarify the competing model paradigms and their interpretation.

1. Introduction

Static and dynamic properties of passive hydraulic engine mounts have been widely studied using experimental and analytical methods [1–12] but their incorporation into system models (such as Fig. 1(a) that depicts a simple vehicle model at low frequencies) is not well understood and somewhat open to interpretation for several reasons. First, mounts are typically characterized by a non-resonant (electro-hydraulic) dynamic test in terms of the dynamic transfer stiffness $K(\omega, X) = F_T/X$ at given angular excitation frequency ω (rad/s) and displacement amplitude X, under a specific static load f_s (or displacement); here F_T is the force transmitted to the blocked base at ω only though other frequencies might be present. Second, mathematical simulations of the mount (alone) are usually developed using lumped fluid models [6,7], such as the one shown in Fig. 1(b). True mechanical (or visco-elastic) analogs of either experimental or analytical treatment cannot be found. Yet, researchers and practitioners have adopted some simplified or even "user friendly" treatments. The chief goal of this communication is to comparatively evaluate competing models at low frequencies (up to 50 Hz) by assuming that the mount (as a component) behaves as a linear time-invariant system. We will also compare the system response properties on the basis of eigensolutions, and frequency and impulse responses in order to clarify some paradoxes or paradigms.

Fig. 1 illustrates competing approaches based on fluid models, analogous mechanical models [1–3], and transfer function formulations [1–6]. In the context of a simplified engine-mount-chassis system, m_e and m_c are the masses of engine and chassis, respectively; k_c and c_c are the stiffness and damping coefficient of chassis; x_e

*Corresponding author. Tel.: +1 614 292 9044; fax: +1 614 292 3163.
E-mail address: singh.3@osu.edu (R. Singh).

0022-460X/$ - see front matter © 2007 Elsevier Ltd. All rights reserved.
doi:10.1016/j.jsv.2007.10.021

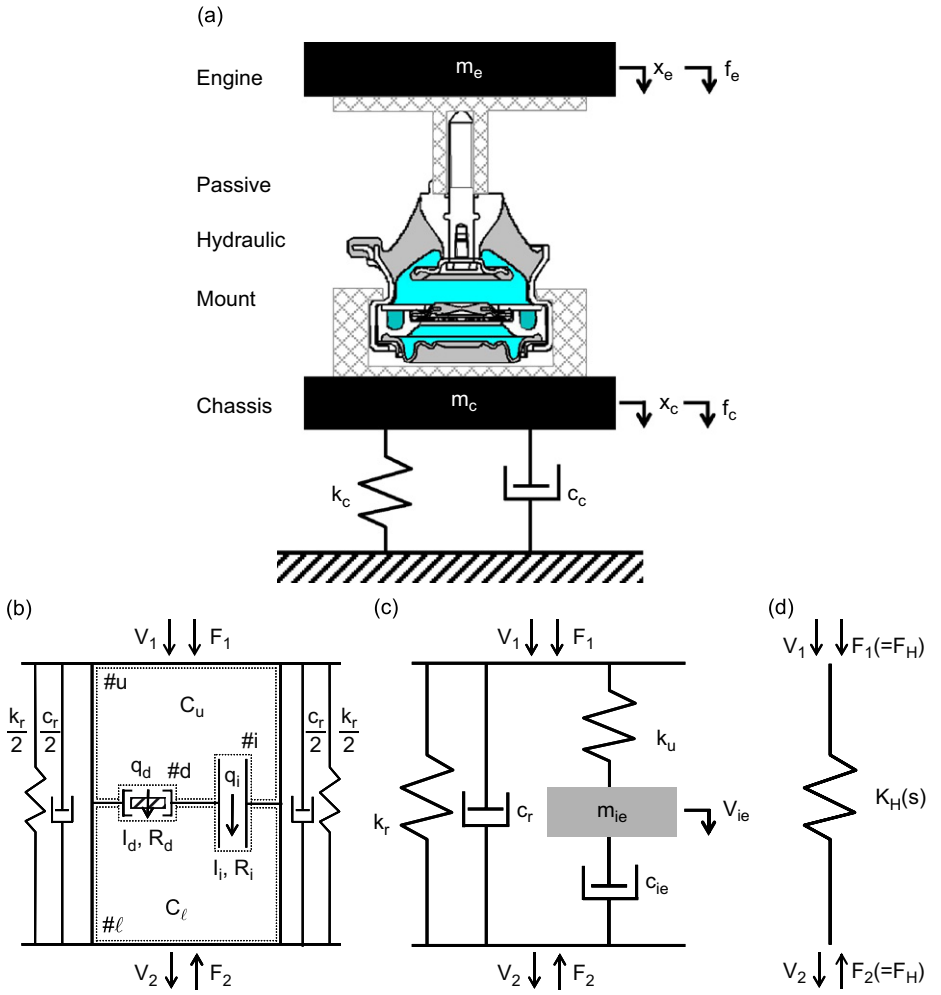

Fig. 1. Engine-mount-chassis system and competing mount models: (a) engine-mount-chassis system, (b) fluid model, (c) mechanical model, (d) transfer function model.

and x_c are the displacements of engine and chassis; f_e and f_c are the forces applied to engine and chassis. For the fluid model in Fig. 1(b), k_r and c_r are the stiffness and damping coefficient of the rubber part, respectively; C_u and C_ℓ are the (linearized) fluid compliances of upper ($\sharp u$) and lower ($\sharp \ell$) chambers; $q_i(t)$ and $q_d(t)$ are the volumetric flow rates through the inertia track ($\sharp i$) and decoupler ($\sharp d$); I_i and I_d are the inertias of fluid columns; R_i and R_d are the (linearized) fluid resistances.

2. Some unique aspects of hydraulic mounts (at low frequencies)

Fig. 2 shows the transfer stiffness of the hydraulic mount measured (solid line) under a large amplitude excitation of 2.0 mm (peak to peak) while being subject to a specific static load corresponding to the engine weight, where strongly spectrally-varying stiffness and damping characteristics due to the so-called inertia track dynamics [8] can be observed. Dashed lines in Fig. 2 represent the predictions based on the following stiffness formulation in the Laplace (s) domain (with three zeros given by z's and two poles given by p's at low frequencies) where α is a real-valued constant.

$$K_H(s) = \alpha \frac{(s - z_1)(s - z_2)(s - z_3)}{(s - p_1)(s - p_2)}. \tag{1}$$

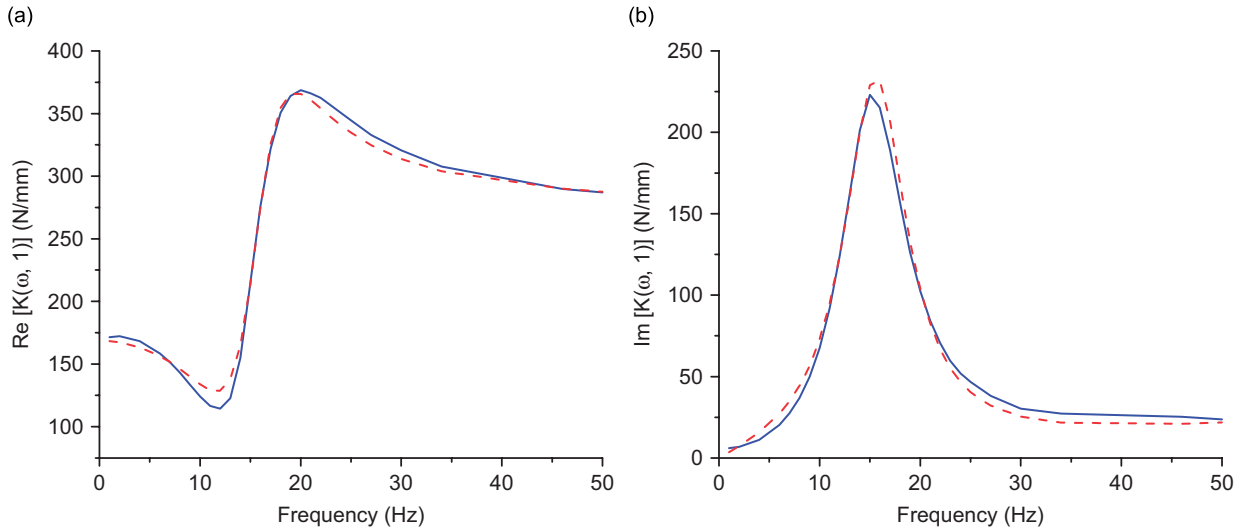

Fig. 2. Measurement of complex-valued transfer stiffness of a typical hydraulic mount: (a) real part, (b) imaginary part. Key: — measurement; –– prediction based on Eq. (1).

Observe that Eq. (1) is in excellent agreement with measurements. Generally, complex poles suggest that the conventional isolator has an embedded mass element. It is in accord with the fact that the fluid mass in the inertia track plays a crucial role in the low-frequency dynamics [9]. However, dynamic response of hydraulic mounts is quite different from that of a conventional mechanical isolator (consisting of spring, dashpot and mass elements). Yet, one of the key features of a massless isolator is that the magnitudes of forces at its input and output sides remain unchanged and thus the conventional isolators (consisting of any combinations of only springs and dashpots) must retain the stiffness matrix in the same form as long as no mass element is included. In other words, an isolator can always be regarded as a spring of equivalent stiffness K_{eq}. Paradoxically, typical hydraulic mount tends to behave like a spring element of equivalent stiffness even though they possess complex poles. For instance, the measurements [9] of four elements of the stiffness matrix, K_{11}, K_{12}, K_{21}, and K_{22}, for the hydraulic mount (as shown below) indicate that it behaves like a spring of equivalent stiffness $K_H(s)$ where 1 and 2 refer to the input and output ends respectively as shown in Fig. 1(d).

$$\mathbf{K} = \begin{bmatrix} K_{11} & K_{12} \\ K_{21} & K_{22} \end{bmatrix} = K_H(s) \begin{bmatrix} 1 & -1 \\ -1 & 1 \end{bmatrix}. \tag{2}$$

3. Features of an analogous mechanical isolator with a mass element

Several mechanical models like Fig. 1(c), or their variants, have been employed to represent strongly frequency-dependent characteristics of hydraulic mounts. In Fig. 1(c), F and V are the force and velocity amplitudes at ω, respectively, and subscripts 1 and 2 mean the input and output ends. The force sign at the output end is opposite to that of the conventional mechanical four-pole parameter theory [13] so that its stiffness matrix can be brought to the same form as Eq. (2) in terms of equivalent stiffness of the isolator. The constraint forces at the input and output ends (at ω) are as follows where $\mathrm{j} = \sqrt{-1}$:

$$F_1 = \left(\frac{k_r}{\mathrm{j}\omega} + c_r\right)(V_1 - V_2) + \frac{k_u}{\mathrm{j}\omega}(V_1 - V_{ie}), \tag{3}$$

$$F_2 = \left(\frac{k_r}{\mathrm{j}\omega} + c_r\right)(V_2 - V_1) + c_{ie}(V_2 - V_{ie}). \tag{4}$$

And the governing equation of the mass element (at ω) is expressed as follows where k_u, m_{ie}, and c_{ie} are, respectively, defined as $k_u = A_p^2/C_u$, $m_{ie} = A_p^2 I_i$, $c_{ie} = A_p^2 R_i$ [10]; here A_p is the effective rubber (piston) area:

$$\mathrm{j}\omega m_{ie} V_{ie} + c_{ie}(V_{ie} - V_2) + \frac{k_u}{\mathrm{j}\omega}(V_{ie} - V_1) = 0. \tag{5}$$

Combining Eqs. (3)–(5) leads to $F_1 = -F_2 + \mathrm{j}\omega m_{ie} V_{ie}$. That is the magnitude of force at the input end of an isolator (with at least one mass element). Therefore, the mechanical model with a lumped mass (m_{ie}) cannot be given by an equivalent stiffness matrix of Eq. (2). Actually, the stiffness matrix of the mechanical model is written as follows:

$$\mathbf{K} = \begin{bmatrix} k_r + \mathrm{j}\omega c_r + k_u \dfrac{\mathrm{j}\omega c_{ie} - \omega^2 m_{ie}}{k_u - \omega^2 m_{ie} + \mathrm{j}\omega c_{ie}} & -\left(k_r + \mathrm{j}\omega c_r + \dfrac{\mathrm{j}\omega c_{ie} k_u}{k_u - \omega^2 m_{ie} + \mathrm{j}\omega c_{ie}}\right) \\ -\left(k_r + \mathrm{j}\omega c_r + \dfrac{\mathrm{j}\omega c_{ie} k_u}{k_u - \omega^2 m_{ie} + \mathrm{j}\omega c_{ie}}\right) & k_r + \mathrm{j}\omega c_r + \mathrm{j}\omega c_{ie} \dfrac{k_u - \omega^2 m_{ie}}{k_u - \omega^2 m_{ie} + \mathrm{j}\omega c_{ie}} \end{bmatrix}. \tag{6}$$

Eq. (6) clearly shows that one transfer stiffness term (K_{12} or K_{21}) is not sufficient to represent the dynamic behavior of an isolator with a lumped mass. The four-pole parameters are also expressed as

$$\begin{Bmatrix} F_1 \\ V_1 \end{Bmatrix} = \begin{bmatrix} \alpha_{11} & \alpha_{12} \\ \alpha_{21} & \alpha_{22} \end{bmatrix} \begin{Bmatrix} F_2 \\ V_2 \end{Bmatrix}$$

$$= \frac{\begin{bmatrix} -\begin{pmatrix} (k_r + \mathrm{j}\omega c_r)(k_u - \omega^2 m_{ie} + \mathrm{j}\omega c_{ie}) \\ +k_u(\mathrm{j}\omega c_{ie} - \omega^2 m_{ie}) \end{pmatrix} & \mathrm{j}\omega m_{ie} \begin{pmatrix} (k_r + \mathrm{j}\omega c_r)(k_u + \mathrm{j}\omega c_{ie}) \\ +\mathrm{j}\omega c_{ie} k_u \end{pmatrix} \\ -\mathrm{j}\omega(k_u - \omega^2 m_{ie} + \mathrm{j}\omega c_{ie}) & \begin{pmatrix} (k_r + \mathrm{j}\omega c_r)(k_u - \omega^2 m_{ie} + \mathrm{j}\omega c_{ie}) \\ +\mathrm{j}\omega c_{ie}(k_u - \omega^2 m_{ie}) \end{pmatrix} \end{bmatrix}}{(k_r + \mathrm{j}\omega c_r)(k_u - \omega^2 m_{ie} + \mathrm{j}\omega c_{ie}) + \mathrm{j}\omega c_{ie} k_u} \begin{Bmatrix} F_2 \\ V_2 \end{Bmatrix}. \tag{7}$$

Observe in Eq. (7) that the mechanical model shows an asymmetry, given by $-\alpha_{11} \neq \alpha_{22}$. In contrast, the hydraulic mount displays symmetry, i.e. the mount behaves in the same way when its input (1) and output (2) ends are interchanged. Accordingly, it should be noted that the mechanical model is not true equivalent of the hydraulic mount even though their driving-point stiffness expressions on the input side are identical.

4. Vehicle system example and conclusion

When both ends of the mount move in a dynamic system, an analogous mechanical model could transmit the wrong force. Further, the modal analysis might not be correct [10]. To critically examine whether the analogous mechanical models can faithfully represent dynamic response of any hydraulic mount, consider the system of Figs. 1(a) and (c). The governing equations are as follows where the subscript M denotes the mechanical model:

$$\mathbf{M}_M \ddot{\mathbf{x}}_M + \mathbf{C}_M \dot{\mathbf{x}}_M + \mathbf{K}_M \mathbf{x}_M = \mathbf{f}_M, \tag{8a}$$

where the matrices $\mathbf{M}_M$, $\mathbf{C}_M$, $\mathbf{K}_M$, and the vectors $\mathbf{x}_M$ and $\mathbf{f}_M$ are defined as

$$\mathbf{M}_M = \begin{bmatrix} m_c & 0 & 0 \\ 0 & m_e & 0 \\ 0 & 0 & m_{ie} \end{bmatrix}, \tag{8b}$$

$$\mathbf{C}_M = \begin{bmatrix} c_c + c_r + c_{ie} & -c_r & -c_{ie} \\ -c_r & c_r & 0 \\ -c_{ie} & 0 & c_{ie} \end{bmatrix}, \tag{8c}$$

$$\mathbf{K}_M = \begin{bmatrix} k_c + k_r & -k_r & 0 \\ -k_r & k_r + k_u & -k_u \\ 0 & -k_u & k_u \end{bmatrix}, \tag{8d}$$

$$\mathbf{x}_M = \begin{Bmatrix} x_c \\ x_e \\ x_{ie} \end{Bmatrix}, \tag{8e}$$

$$\mathbf{f}_M = \begin{Bmatrix} f_c \\ f_e \\ 0 \end{Bmatrix}. \tag{8f}$$

Next, consider the system of Figs. 1(a) and (d) that incorporates the transfer function model of the hydraulic mount (based on the fluid formulation or complete measured data). Introduce an internal force f_H of a spring of equivalent stiffness $K_H(s)$ and write the corresponding equations of motion and associated matrices or vectors (with subscript T) as follows; see Appendix A for the expressions of C_{31}, C_{32}, C_{33}, K_{31}, K_{32}, K_{33}, B_{131}, B_{132}, B_{031}, and B_{032} (based on the fluid model).

$$\mathbf{M}_T\ddot{\mathbf{x}}_T + \mathbf{C}_T\dot{\mathbf{x}}_T + \mathbf{K}_T\mathbf{x}_T = \mathbf{B}_1\dot{\mathbf{f}}_T + \mathbf{B}_0\mathbf{f}_T, \tag{9a}$$

$$\mathbf{M}_T = \begin{bmatrix} m_c & 0 & 0 \\ 0 & m_e & 0 \\ 0 & 0 & m_{ie} \end{bmatrix}, \tag{9b}$$

$$\mathbf{C}_T = \begin{bmatrix} c_c & 0 & 0 \\ 0 & 0 & 0 \\ C_{31} & C_{32} & C_{33} \end{bmatrix}, \tag{9c}$$

$$\mathbf{K}_T = \begin{bmatrix} k_c & 0 & -1 \\ 0 & 0 & 1 \\ K_{31} & K_{32} & K_{33} \end{bmatrix}, \tag{9d}$$

$$\mathbf{B}_1 = \begin{bmatrix} 0 & 0 \\ 0 & 0 \\ B_{131} & B_{132} \end{bmatrix} = \begin{bmatrix} \mathbf{B}_{11} & \mathbf{B}_{12} \end{bmatrix}, \tag{9e}$$

$$\mathbf{B}_0 = \begin{bmatrix} 1 & 0 \\ 0 & 1 \\ B_{031} & B_{032} \end{bmatrix} = \begin{bmatrix} \mathbf{B}_{01} & \mathbf{B}_{02} \end{bmatrix}, \tag{9f}$$

$$\mathbf{x}_T = \begin{Bmatrix} x_c \\ x_e \\ f_H \end{Bmatrix}, \tag{9g}$$

$$\mathbf{f}_T = \begin{Bmatrix} f_c \\ f_e \end{Bmatrix}. \tag{9h}$$

By solving the complex eigenvalue problem of dimension 6, the frequency response functions (H_{rq}), at the rth coordinate due to unit Gaussian (White) random excitation at the qth coordinate with no other inputs at

any other coordinates, are written as follows for the models of Figs. 1(c) and (d) using subscripts M and T, respectively [14]:

$$H_{Mrq}(\omega) = \sum_{i=1}^{6} \frac{v_{Miq} u_{Mir}}{\mathrm{j}\omega - \lambda_{Mi}}, \tag{10a}$$

$$H_{Trq}(\omega) = \sum_{i=1}^{6} \frac{\mathrm{j}\omega}{\mathrm{j}\omega - \lambda_{Ti}} (\mathbf{v}_{Ti}^{\mathrm{T}} \mathbf{B}_{1q}) u_{Tir} + \sum_{i=1}^{6} \frac{1}{j\omega - \lambda_{Ti}} (\mathbf{v}_{Ti}^{\mathrm{T}} \mathbf{B}_{0q}) u_{Tir}, \tag{10b}$$

where λ_i is the ith eigenvalue, v_{iq} is the qth element of the ith left eigenvector $\mathbf{v}_i$ and u_{ir} is the rth element of the ith right eigenvector $\mathbf{u}_i$; $\mathbf{B}_{1q}$ and $\mathbf{B}_{0q}$ are the qth column vectors of $\mathbf{B}_1$ and $\mathbf{B}_0$, respectively. The superscript T denotes the transpose. The terms with $\mathbf{B}_{1q}$ can be easily derived from the corresponding terms with $\mathbf{B}_{0q}$ by differentiation. The corresponding impulse response functions for both models are expressed as follows where

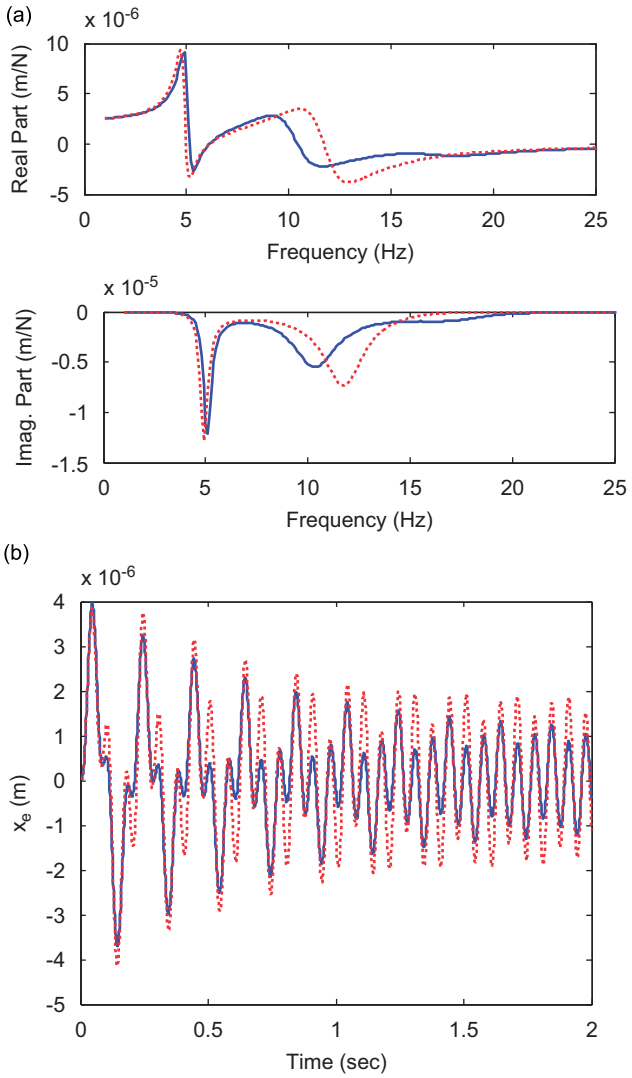

Fig. 3. System responses obtained by using mechanical and transfer function models: (a) frequency response spectra (X_c/F_c) (ω), (b) harmonic response $x_e(t)$. Key: — transfer function model of Fig. 1(d); –– mechanical model of Fig. 1(c).

$U(t)$ is the unit step function and $\delta(t)$ is the Dirac delta function.

$$h_{Mrq}(t) = \sum_{i=1}^{6} v_{Miq} u_{Mir} e^{\lambda_{Mi} t} U(t),$$

$$h_{Trq}(t) = \sum_{i=1}^{6} (\mathbf{v}_{Ti}^{\mathrm{T}} \mathbf{B}_{1q}) u_{Tir} \{\lambda_{Ti} U(t) + \delta(t)\} e^{\lambda_{Ti} t} + \sum_{i=1}^{6} (\mathbf{v}_{Ti}^{\mathrm{T}} \mathbf{B}_{0q}) u_{Tir} e^{\lambda_{Ti} t} U(t).$$

Further, if the harmonic excitation at ω_0 rad/s in the form of $\sin(\omega_0 t)U(t)$ were to be applied to the engine m_e, the harmonic responses for both models would yield by convolution integral:

$$x_{eM}(t) = \sum_{i=1}^{6} v_{Mi2} u_{Mi2} \frac{\omega_0 e^{\lambda_{Mi} t} - \lambda_{Mi} \sin \omega_0 t - \omega_0 \cos \omega_0 t}{\omega_0^2 + \lambda_{Mi}^2} U(t), \tag{11a}$$

$$\begin{aligned} x_{eT}(t) = & \sum_{i=1}^{6} (\mathbf{v}_{Ti}^{\mathrm{T}} \mathbf{B}_{12}) u_{Ti2} \omega_0 \frac{\lambda_{Ti} e^{\lambda_{Ti} t} + \omega_0 \sin \omega_0 t - \lambda_{Ti} \cos \omega_0 t}{\omega_0^2 + \lambda_{Ti}^2} U(t) \\ & + \sum_{i=1}^{6} (\mathbf{v}_{Ti}^{\mathrm{T}} \mathbf{B}_{02}) u_{Ti2} \frac{\omega_0 e^{\lambda_{Ti} t} - \lambda_{Ti} \sin \omega_0 t - \omega_0 \cos \omega_0 t}{\omega_0^2 + \lambda_{Ti}^2} U(t). \end{aligned} \tag{11b}$$

For the sake of illustration, consider the following typical values: $m_c = 120$ kg, $m_e = 100$ kg, $k_c = 401.1$ N/mm, $c_c = 256$ N s/m, $m_{ie} = 11.9$ kg, $c_{ie} = 492$ N s/m, $k_r = 167.6$ N/mm, $k_u = 112.2$ N/mm, and $c_r = 146$ N s/m. The resulting complex eigenvalues for both models are: $\lambda_M = -1.38 \pm \mathrm{j}30.8$, $-7.42 \pm \mathrm{j}74.0$, $-16.3 \pm \mathrm{j}99.1$; and, $\lambda_T = -1.42 \pm \mathrm{j}31.8$, $-8.12 \pm \mathrm{j}64.8$, $-13.5 \pm \mathrm{j}110$. Thus, one can confirm that the mechanical model yields the wrong eigensolutions. Fig. 3 shows the frequency response functions (based on Eq. (10)) and harmonic responses at $\omega_0 = 2\pi \cdot 15$ rad/s (based on Eq. (11)). Results clearly show why the mechanical model must not be employed in a system where both ends of the hydraulic mount move. It is noted here that the mechanical model could indeed work if one end of the hydraulic mount is somehow fixed (say to a massive inertial base); this suggests that only the driving-point stiffness of the mechanical model would then dictate the dynamic behavior.

Acknowledgments

This work was supported by the Korea Research Foundation Grant (KRF-2006-352-D00035) funded by the Korean Government (MOEHRD).

Appendix A. Expressions of Eq. (9) for the system of Figs. 1(a) and (d)

$$\begin{aligned} C_{31} &= m_{ie} c_r \frac{c_c^2 - m_c k_c}{m_c^2} - (c_{ie} c_r + k_r m_{ie} + k_u m_{ie}) \frac{c_c}{m_c} + (c_r k_u + k_r c_{ie} + k_u c_{ie}), \\ C_{32} &= -(c_r k_u + k_r c_{ie} + k_u c_{ie}), \quad C_{33} = c_{ie} + m_{ie} c_r \left(\frac{1}{m_c} + \frac{1}{m_e} \right), \end{aligned} \tag{A.1}$$

$$\begin{aligned} K_{31} &= m_{ie} c_r \frac{c_c k_c}{m_c^2} + k_r k_u - (c_{ie} c_r + k_r m_{ie} + k_u m_{ie}) \frac{k_c}{m_c}, \\ K_{32} &= -k_r k_u, \quad K_{33} = k_u - c_c c_r \frac{m_{ie}}{m_c^2} + (c_{ie} c_r + k_r m_{ie} + k_u m_{ie}) \left(\frac{1}{m_c} + \frac{1}{m_e} \right), \end{aligned} \tag{A.2}$$

$$B_{131} = -\frac{m_{ie}c_r}{m_c}, \quad B_{132} = \frac{m_{ie}c_r}{m_e},$$
$$B_{031} = \frac{m_{ie}c_rc_c}{m_c^2} - \frac{c_{ie}c_r + k_rm_{ie} + k_um_{ie}}{m_c}, \quad B_{032} = \frac{c_{ie}c_r + k_rm_{ie} + k_um_{ie}}{m_e}. \tag{A.3}$$

References

[1] R. Singh, G. Kim, P.V. Ravindra, Linear analysis of automotive hydro-mechanical mount with emphasis on decoupler characteristics, *Journal of Sound and Vibration* 158 (1992) 219–243.

[2] J.E. Colgate, C.-T. Chang, Y.-C. Chiou, W.K. Liu, L.M. Keer, Modelling of a hydraulic engine mount focusing on response to sinusoidal and composite excitations, *Journal of Sound and Vibration* 184 (1995) 503–528.

[3] G.N. Jazar, M.F. Golnaraghi, Nonlinear modeling, experimental verification, and theoretical analysis of a hydraulic engine mount, *Journal of Vibration and Control* 8 (2002) 87–116.

[4] T. Jeong, R. Singh, Inclusion of measured frequency- and amplitude-dependent mount properties in vehicle or machinery models, *Journal of Sound and Vibration* 245 (2001) 385–415.

[5] M.S. Foumani, A. Khajepour, M. Durali, Application of sensitivity analysis to the development of high performance adaptive hydraulic engine mounts, *Vehicle System Dynamics* 39 (2003) 257–278.

[6] H. Adiguna, M. Tiwari, R. Singh, H.E. Tseng, D. Hrovat, Transient response of a hydraulic engine mount, *Journal of Sound and Vibration* 268 (2003) 217–248.

[7] M. Tiwari, H. Adiguna, R. Singh, Experimental characterization of a nonlinear hydraulic engine mount, *Noise Control Engineering Journal* 51 (2003) 36–49.

[8] J.-H. Lee, K.-J. Kim, An efficient technique for design of hydraulic engine mount via design variable-embedded damping modeling, *Journal of Vibration and Acoustics* 127 (2005) 93–99.

[9] J.-H. Lee, M.-S. Bae, K.-J. Kim, Limitations of mechanical model with lumped mass in representing dynamic characteristics of hydraulic mount (SAE 2003-01-1466), *Journal of Passenger Cars—Mechanical Systems* 112 (2004) 1679–1683.

[10] S. He, R. Singh, Incorporation of non-linear and quasi-linear hydraulic mount formulations into a vehicle model, *2007 SAE Noise and Vibration Conference*, St. Charles, IL, 2007-01-2367.

[11] W.-B. Shangguan, Z.-H. Lu, Modelling of a hydraulic engine mount with fluid-structure interaction finite element analysis, *Journal of Sound and Vibration* 275 (2004) 193–221.

[12] W.-B. Shangguan, Z.-H. Lu, Experimental study and simulation of a hydraulic engine mount with fully-structure interaction finite element analysis model, *Computers and Structures* 82 (22) (2004) 1751–1771.

[13] J.C. Snowdon, Mechanical four-pole parameters and their application, *Journal of Sound and Vibration* 15 (3) (1971) 307–323.

[14] S.-W. Hong, C.-W. Lee, Frequency and time domain analysis of linear systems with frequency dependent parameters, *Journal of Sound and Vibration* 127 (2) (1988) 365–378.